Polymerization of Lactide Using Achiral Bis(pyrrolidene) Schiff Base Aluminum Complexes

Hongzhi Du,[†,§,||] Aldrik H. Velders,[‡] Pieter J. Dijkstra,[†] Zhiyuan Zhong,[⊥] Xuesi Chen,*[,§,||] and Jan Feijen*[,†]

Department of Polymer Chemistry and Biomaterials, Faculty of Science and Technology, Institute for Biomedical Technology and Laboratory of Supramolecular Chemistry and Technology, MESA+ Research Institute, University of Twente, 7500 AE Enschede, The Netherlands, State Key Laboratory of Polymer Physics and Chemistry, Changchun Institute of Applied Chemistry, Chinese Academy of Sciences, Changchun 130022, China, Graduate School, Chinese Academy of Sciences, Beijing 100039, China, and Biomedical Polymers Laboratory and Jiangsu Key Laboratory of Organic Chemistry, College of Chemistry, Chemical Engineering and Materials Science, Soochow University, Suzhou 215123, P.R. China

Received November 14, 2008; Revised Manuscript Received December 15, 2008

ABSTRACT: A series of aluminum ethyls and isopropoxides based on a bis(pyrrolidene) Schiff base ligand framework has been prepared and characterized. NMR studies of the dissolved complexes indicate that they adopt a symmetric structure with a monomeric, five-coordinated aluminum center core. The aluminum ethyls used as catalysts in the presence of 2-propanol as initiator and the aluminum isopropoxides were applied for lactide polymerization in toluene to test their activities and stereoselectivities. All polymerizations are living, as evidenced by the narrow polydispersities and the good fit between calculated and found number-average molecular weights of the isolated polymers. All of these aluminum complexes polymerized (*S*,*S*)-lactide to highly isotactic PLA without epimerization of the monomer, furnished isotactic-biased polymer from *rac*-lactide, and gave atactic polymer from *meso*-lactide. The study of kinetics indicated that the activity of the bis(pyrrolidene) Schiff base aluminum initiator systems toward lactide polymerization decreases in the following order: (*S*,*S*)-lactide > *rac*-lactide > *meso*-lactide. The methyl substituents on the diimine bridge or on the pyrrole rings both exert significant influence on the course of the polymerizations, affecting both the stereoselectivity and the polymerization rate. Kinetics using [L^2AlEt]/2-propanol (**2a**/2-propanol) and [L^2AlO^{i}Pr] (**2b**) indicated that the polymerizations are both first-order with respect to *rac*-lactide monomer and catalyst. The higher polymerization rate constant (k_p) values for [L^2AlO^{i}Pr] (**2b**) compared with those of [L^2AlEt]/2-propanol (**2a**/2-propanol) revealed that in this case the overall polymerization rate was influenced by the relatively slow in situ alcoholysis reaction of aluminum ethyls. Polymerization experiments with [L^2AlO^{i}Pr] (**2b**) revealed that with this complex much faster (k_p = 13.0 L·mol^{-1}·min^{-1}) lactide polymerizations can be achieved compared with other aluminum complexes.

Introduction

Poly(lactic acid)s (PLAs) have been intensively studied during the past decades, because of their biodegradability and biocompatibility, which give them potential applications in environmental, biomedical, and pharmaceutical fields.[1] PLAs are usually prepared by ring-opening polymerization of lactide (LA), a cyclic dimer of lactic acid, generally applying metal-based catalysis. A large number of nonligated metal complexes, in particular, metal alkoxides of Al,[2] Li,[3] Ca,[4] Fe,[5] Sn,[6] Zn,[7] and Ln,[8] have been explored for these purposes. Problems associated with the use of some of these nonligated metal alkoxides are racemization and transesterification as side reactions during the polymerization, which lead to the disturbance of the polymer microstructure, unpredictable molecular weights as well as a broad molecular weight distributions, and the formation of macrocycles or low-molecular-weight oligomers.[9]

Metal ion complexes in which the metal ion is coordinated with one alkoxide group and a multidentate ligand containing heteroatoms are efficient catalyst-initiator systems for the ring-opening polymerization of lactones. These complexes are so-called single-site metal catalysts with the formula L_nMR, where L_n represents the ancillary ligand, M represents the central metal atom, and R is the initiating group.[10] Using such single-site metal catalysts with appropriate combinations of L_n, M, and R, PLAs with a predicted molecular weight and narrow molecular weight distributions can be prepared. Moreover, PLAs with a high tacticity become available from the ring-opening polymerization of *rac*-LA (a 1:1 mixture of (*S*,*S*)-LA and (*R*,*R*)-LA) or *meso*-LA.[11]

Many single-site catalysts comprising zinc[12] and magnesium[13] alkoxides stabilized by β-diketiminate ligand, aluminum complexes[14] supported by fluorinated dialkoxy-diimino ligands, germanium,[15] titanium,[16] and lanthanide[17] complexes ligated by mono- or multiphenolates have been proven to be efficient initiator/catalyst systems that give a well controlled and stereoselective polymerization of LAs. The five-coordinated aluminum alkoxides supported by *N*,*N*,*O*,*O*-tetradentate salicylaldehyde Schiff base ligands occupy an important position among these catalysts. Because Spassky and coworkers have found that enantiomerically pure (*R*)-(SalBinap)-AlOCH$_3$ exhibited a 20:1 preference for the polymerization of (*R*,*R*)-LA over (*S*,*S*)-LA, leading to a tapered stereoblock microstructure,[18] many achiral and chiral salicylaldehyde Schiff base aluminum complexes have been reported that furnish highly isotactic, stereoblock PLAs from *rac*-LA via a chain-end-control mechanism[19] or a site-control mechanism[20] and highly syndiotactic PLA material from

* Corresponding authors. E-mail: j.feijen@tnw.utwente.nl (J.F.); xschen@ciac.jl.cn (X.C.).
† Department of Polymer Chemistry and Biomaterials, Faculty of Science and Technology, Institute for Biomedical Technology, University of Twente.
‡ Laboratory of Supramolecular Chemistry and Technology, MESA+ Research Institute, University of Twente.
§ Changchun Institute of Applied Chemistry, Chinese Academy of Sciences.
|| Graduate School, Chinese Academy of Sciences.
⊥ Soochow University.

10.1021/ma802564s CCC: $40.75
Published on Web 01/23/2009

meso-LA through a site-control mechanism.[20b] Recent studies reported by Gibson and us have re-evaluated the achiral Schiff base aluminum catalyst system to show the steric and electronic factors that influence the polymerization rate and stereoselectivity.[21] However, almost all Schiff base aluminum catalysts derived from salicylaldehyde do not have a high activity in LA polymerization, and the polymerization rates are much lower than those for the other reported metal catalyst systems.

Compared with the existing aluminum catalysts with a five-coordinated salicylaldehyde Schiff base ligand system, which have a high tacticity control toward *rac*-LA polymerization, the use of five-coordinated aluminum catalysts ligated by bis(pyrrolidene) Schiff base ligands in the ring-opening polymerizations of LA has not been disclosed. Here we report the synthesis of a series of aluminum ethyls and corresponding isopropoxides based on bis(pyrrolidene) Schiff base ligands. The stereoselectivity of in situ-formed aluminum isopropoxides from the corresponding aluminum ethyls toward *rac*-LA and *meso*-LA as well as the kinetics of the ring-opening polymerization of *rac*-LA, *meso*-LA, and (*S*,*S*)-LA with these systems were determined.

Experimental Section

General. All experiments were carried out under a dry nitrogen atmosphere using standard Schlenk techniques or in a glovebox. Toluene and hexane were distilled from Na-benzophenone before use. A 25 wt % solution of triethylaluminum in toluene (Aldrich) was used without prior purification. 1,3-Propanediamine (99%), 2,2-dimethyl-1,3-propanediamine (99%), pyrrole-2-carboxaldehyde (98%), and 3,5-dimethylpyrrole-2-carboxaldehyde (95%) from Aldrich were used without further purification. The monomers (*S*,*S*)-LA, *rac*-LA, and *meso*-LA (Purac Biochem b.v., The Netherlands) were purified two times by recrystallization from dry toluene and dried under vacuum. All glassware was dried in an oven before use.

1D ^{1}H (300 MHz) and ^{13}C (75 MHz) nuclear magnetic resonance (NMR) spectra were recorded on a Varian Unity 300 NMR spectrometer using $CDCl_3$ solutions at 298 K and were referenced to shifts of residual $CHCl_3$ (δ = 7.26 for ^{1}H NMR and 77.0 for ^{13}C NMR). Homonuclear decoupled ^{1}H NMR, ^{1}H−^{1}H COSY, ^{1}H−^{1}H NOESY, and diffusion-ordered spectroscopy (DOSY) spectra were recorded on a Bruker Avance II 600 MHz spectrometer operating at 600.13 MHz at 295 K, and variable temperature (VT) ^{1}H NMR spectra were recorded on the same Bruker Avance II 600.13 MHz spectrometer in the temperature range of 295−360 K. The spectrometer was equipped with a Great 3/10 gradient amplifier and a triple-nucleus TXI probe with z gradient. All experiments were performed using standard pulse sequences from the Bruker library. Pulsed field gradient stimulated echo (PFGSE) diffusion experiments were performed using the bipolar stimulated echo sequence with 32 increments in the gradient strength (2−95%), typically 16 averages per increment step, and 100 ms diffusion time. Gel permeation chromatography (GPC) measurements were conducted with a Waters 410 GPC with tetrahydrofuran (THF) as the eluent (flow rate: 1 mL·min^{-1} at 35 °C). The molecular weights were calibrated against polystyrene (PS) standards. Matrix-assisted laser desorption ionization time-of-flight (MALDI-TOF) mass spectrometry using a Voyager-DE-RP MALDI-TOF mass spectrometer (Applied Biosystems/PerSeptive Biosystems, Framingham, MA) equipped with delayed extraction. A 337 nm UV nitrogen laser producing 4 ns pulses was used, and the mass spectra were obtained in the linear and reflection modes.

Synthesis of Ligands. *Synthesis of 1,3-Bis(pyrrole-2-yl-methyleneamine)propane (**H$_2$L^1**).* Pyrrole-2-carboxaldehyde (1.90 g, 20 mmol) and 1,3-propanediamine (0.74 g, 10 mmol) were dissolved in 10 mL of methanol. The mixture was stirred, and a catalytic amount of glacial acetic acid was added. After a few seconds, a white precipitate was formed. The suspension was allowed to be stirred at room temperature for 2 h. The white solid was collected by filtration, washed with cold methanol, and dried under vacuum to produce the pure product. Yield: 1.78 g (78%). ^{1}H NMR (300 MHz, $CDCl_3$, 25 °C, δ): 8.05 (s, 2H, $N=CH$), 6.87 (d, J_{H-H} = 1.2 Hz, 2H, pyrrole-*H*), 6.46 (dd, J_{H-H} = 1.5 Hz, J_{H-H} = 3.6 Hz, 2H, pyrrole-*H*), 6.23 (dd, J_{H-H} = 3.0 Hz, J_{H-H} = 3.6 Hz, 2H, pyrrole-*H*), 3.60 (td, 4H, J_{H-H} = 1.2 Hz, J_{H-H} = 7.2 Hz, NCH_2), 1.98 (t, 2H, J_{H-H} = 6.6 Hz, CH_2CH_2 CH_2). ^{13}C NMR (75 MHz, $CDCl_3$, 25 °C, δ): 152.3 (*C*H═N), 130.1, 122.0, 114.3, 109.5 (pyrrole-*C*), 58.1 (NCH_2), 32.6 ($CH_2CH_2CH_2$). Anal. Calcd for $C_{13}H_{16}N_4$: C, 68.39; H, 7.06; N, 24.54. Found: C, 68.10; H, 6.89; N, 24.87.

*Synthesis of 2,2-Dimethyl-1,3-bis(pyrrole-2-yl-methyleneamine)propane (**H$_2$L^2**).* The method is similar to that used for **H$_2$L^1** except that 2,2-dimethyl-1,3-propane-diamine (1.02 g, 10 mmol) was used as reagent. Yield: 76%. ^{1}H NMR (300 MHz, $CDCl_3$, 25 °C, δ): 7.98 (s, 2H, $N=CH$), 6.90 (s, 2H, pyrrole-*H*), 6.46 (dd, J_{H-H} = 1.5 Hz, J_{H-H} = 3.6 Hz, 2H, pyrrole-*H*), 6.24 (dd, J_{H-H} = 2.4 Hz, J_{H-H} = 3.9 Hz, 2H, pyrrole-*H*), 3.41 (d, J_{H-H} = 1.2 Hz, 4H, NCH_2), 0.97 (s, 6H, $C(CH_3)_2$). ^{13}C NMR (75 MHz, $CDCl_3$, 25 °C, δ): 152.2 (*C*H═N), 130.4, 122.1, 114.2, 109.5 (pyrrole-*C*), 69.7 (NCH_2), 37.2 ($C(CH_3)_2$), 24.4 ($C(CH_3)_2$). Anal. Calcd for $C_{15}H_{20}N_4$: C, 70.28; H, 7.86; N, 21.86. Found: C, 70.07; H, 8.01; N, 21.97.

*Synthesis of 2,2-Dimethyl-1,3-bis(3,5-dimethyl-pyrrole-2-yl-methyleneamine) Propane (**H$_2$L^3**).* The method is similar to that used for **H$_2$L^1** except that 3,5-dimethylpyrrole-2-carboxaldehyde (2.46 g, 20 mmol) and 2,2-dimethyl-1,3-propanediamine (1.02 g, 10 mmol) were used as reagents. Yield: 75%. ^{1}H NMR (300 MHz, $CDCl_3$, 25 °C, δ): 8.00 (s, 2H, $N=CH$), 5.73 (s, 2H, pyrrole-*H*), 3.37 (s, 4H, NCH_2), 2.23 (s, 6H, pyrrole-CH_3), 2.14 (s, 6H, pyrrole-CH_3), 0.97 (s, 6H, $C(CH_3)_2$). ^{13}C NMR (75 MHz, $CDCl_3$, 25 °C, δ): 149.9 (*C*H═N), 131.4, 125.4, 124.4, 109, 7 (pyrrole-*C*), 70.3 (NCH_2), 37.1 ($C(CH_3)_2$), 24.5 ($C(CH_3)_2$), 13.0 (pyrrole-CH_3), 10.4 (pyrrole-CH_3). Anal. Calcd for $C_{19}H_{28}N_4$: C, 73.04; H, 9.03; N, 17.93. Found: C, 73.21; H, 8.97; N, 18.27.

Synthesis of Complexes. *Synthesis of [L^{1}AlEt] (**1a**).* Triethylaluminum (0.10 g, 0.88 mmol) in 3 mL of toluene was added to a suspension of **H$_2$L^1** (0.20 g, 0.88 mmol) in 1 mL of toluene. After being stirred for 2 h at room temperature, the mixture was heated to 70 °C for another 2 h. The white precipitate was filtered, washed with hexane, and subsequently dried under vacuum for 24 h. An analytical pure product was obtained in 82% yield. ^{1}H NMR (300 MHz, $CDCl_3$, 25 °C, δ): 8.08 (s, 2H, $N=CH$), 7.53 (d, J_{H-H} = 1.8 Hz, 2H, pyrrole-*H*), 6.85 (dd, J_{H-H} = 0.6 Hz, J_{H-H} = 3.3 Hz, 2H, pyrrole-*H*), 6.50 (dd, J_{H-H} = 1.8 Hz, J_{H-H} = 3.3 Hz, 2H, pyrrole-*H*), 3.86 (d, 2H, NCH_2), 3.75 (d, 2H, NCH_2), 2.10 (s, 1H, $CH_2CH_2CH_2$), 1.89 (s, 1H, $CH_2CH_2CH_2$), 0.80 (t, 3H, $AlCH_2CH_3$), −0.15 (q, 2H, $AlCH_2CH_3$). ^{13}C NMR data are not available due to the limited solubility of complex [L^{1}AlEt] (**1a**). Anal. Calcd for $C_{15}H_{19}AlN_4$: C, 63.81; H, 6.78; N, 19.85. Found: C, 64.06; H, 7.11; N, 19.37.

*Synthesis of [L^{2}AlEt] (**2a**).* Triethylaluminum (0.089 g, 0.78 mmol) in 5 mL of hexane was added to a solution of **H$_2$L^2** (0.20 g, 0.78 mmol) in 2 mL of toluene. After being stirred for 2 h at room temperature, the mixture was heated to 70 °C for another 2 h. The mixture was slowly cooled to room temperature overnight to yield colorless crystals. After being washed with hexane and subsequently dried under vacuum for 24 h, an analytically pure product was obtained in 71% yield. The ^{1}H and ^{13}C NMR spectra of **2a** are displayed in Figures S1 and S2 in the Supporting Information. ^{1}H NMR (300 MHz, $CDCl_3$, 25 °C, δ): 7.84 (s, 2H, $N=CH$), 7.40 (t, J_{H-H} = 0.6 Hz, 2H, pyrrole-*H*), 6.69 (dd, J_{H-H} = 0.6 Hz, J_{H-H} = 3.6 Hz, 2H, pyrrole-*H*), 6.35 (dd, J_{H-H} = 1.8 Hz, J_{H-H} = 3.6 Hz, 2H, pyrrole-*H*), 3.82 (d, J_{H-H} = 12.0 Hz, 2H, NCH_2), 3.26 (d, J_{H-H} = 12.0 Hz, 2H, NCH_2), 1.06 (s, 3H, $C(CH_3)_2$), 0.89 (s, 3H, $C(CH_3)_2$), 0.82 (t, 3H, $AlCH_2CH_3$), −0.15 (q, 2H, $AlCH_2CH_3$). ^{13}C NMR (75 MHz, $CDCl_3$, 25 °C, δ): 159.1 (*N*=*C*H), 135.4, 134.6, 116.3, 113.5 (pyrrole-*C*), 67.7 (NCH_2), 35.6 ($C(CH_3)_2$), 25.8, 22.1 ($C(CH_3)_2$), 9.1 ($AlCH_2CH_3$), −0.4 ($AlCH_2CH_3$). Anal. Calcd for $C_{17}H_{23}AlN_4$: C, 65.79; H, 7.47; N, 18.05. Found: C, 66.20; H, 7.99; N, 17.92.

*Synthesis of [L^{3}AlEt] (**3a**).* Triethylaluminum (0.073 g, 0.64 mmol) in 4.1 mL of hexane was added to a solution of **H$_2$L^3** (0.20

Scheme 1. Bis(pyrrolidene) Schiff Base Aluminum Ethyls and Isopropoxides

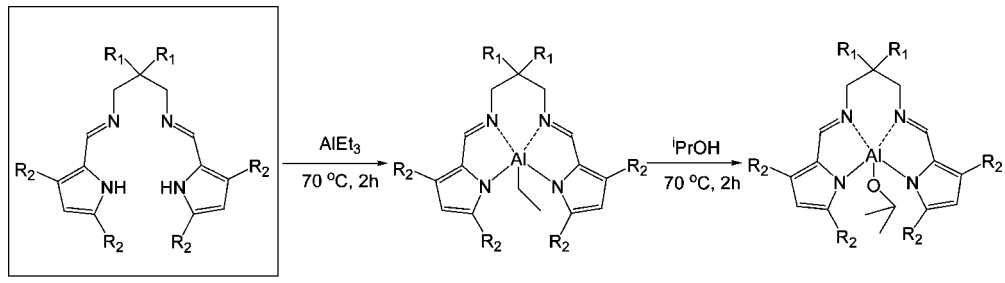

$R_1 = R_2 = H$, H_2L^1; $R_1 = Me, R_2 = H$, H_2L^2; $R_1 = R_2 = Me$, H_2L^3.

$R_1 = R_2 = H$, **1a**; $R_1 = Me, R_2 = H$, **2a**; $R_1 = R_2 = Me$, **3a**.

$R_1 = Me, R_2 = H$, **2b**; $R_1 = R_2 = Me$, **3b**.

g, 0.64 mmol) in 2 mL of toluene. After being stirred for 2 h at room temperature, the mixture was heated to 70 °C for another 2 h. The mixture was slowly cooled to room temperature overnight to yield colorless crystals. After washing with hexane and drying under vacuum for 24 h, an analytical pure product was obtained in 69% yield. The ^{1}H and ^{13}C NMR spectra of **3a** were displayed in Figures S5 and S6 in the Supporting Information. ^{1}H NMR (300 MHz, $CDCl_3$, 25 °C, δ): 7.69 (s, 2H, $N=CH$), 5.84 (s, 2H, pyrrole-*H*), 3.54 (d, $J_{H-H} = 12.0$ Hz, 2H, NCH_2), 3.24 (d, $J_{H-H} = 12.0$ Hz, 2H, NCH_2), 2.17 (s, 6H, pyrrole-CH_3), 2.12 (s, 6H, pyrrole-CH_3), 1.12 (s, 3H, $C(CH_3)_2$), 0.92 (s, 3H, $C(CH_3)_2$), 0.84 (t, 3H, $AlCH_2CH_3$), 0.02 (q, 2H, $AlCH_2CH_3$). ^{13}C NMR (75 MHz, $CDCl_3$, 25 °C, δ): 154.8 ($N=CH$), 147.9, 132.9, 129.9, 115.0 (pyrrole-*C*), 66.1 (NCH_2), 35.8 ($C(CH_3)_2$), 26.5, 25.8 ($C(CH_3)_2$), 15.6 (pyrrole-CH_3), 10.7 (pyrrole-CH_3), 9.7 ($AlCH_2CH_3$), 2.7 ($AlCH_2CH_3$). Anal. Calcd for $C_{21}H_{31}AlN_4$: C, 68.82; H, 8.53; N, 15.29. Found: C, 69.41; H, 8.89; N, 15.02.

*Synthesis of [L^{2}AlO^{i}Pr] (***2b***).* 2-Propanol (0.019 g, 0.32 mmol) in 2 mL of toluene was added to a suspension of [L^{2}AlEt] (**2a**) (0.10 g, 0.32 mmol) in 5 mL of a mixed solution of toluene and hexane (1:3 v/v) at room temperature. After the mixture was stirred for 2 h at 70 °C, it was slowly cooled to room temperature overnight. Colorless crystals were obtained that were filtered and washed with hexane. After drying under vacuum for 24 h, an analytically pure product was obtained in 65% yield. The ^{1}H and ^{13}C NMR spectra of **2b** were displayed in Figures S3 and S4 in the Supporting Information. ^{1}H NMR (300 MHz, $CDCl_3$, 25 °C, δ): 7.82 (s, 2H, $N=CH$), 7.36 (t, $J_{H-H} = 0.6$ Hz, 2H, pyrrole-*H*), 6.67 (dd, $J_{H-H} = 0.6$ Hz, $J_{H-H} = 3.6$ Hz, 2H, pyrrole-*H*), 6.33 (dd, $J_{H-H} = 1.8$ Hz, $J_{H-H} = 3.6$ Hz, 2H, pyrrole-*H*), 3.88 (d, $J_{H-H} = 12.0$ Hz, 2H, NCH_2), 3.79 (m, 1H, $OCH(CH_3)_2$), 3.23 (d, $J_{H-H} = 12.0$ Hz, 2H, NCH_2), 1.07 (s, 3H, $C(CH_3)_2$), 1.00 (m, 6H, $OCH(CH_3)_2$), 0.89 (s, 3H, $C(CH_3)_2$). ^{13}C NMR (75 MHz, $CDCl_3$, 25 °C, δ): 159.8 ($N=CH$), 136.0, 134.4, 117.1, 113.8 (pyrrole-*C*), 67.4 (NCH_2), 62.9 ($OCH(CH_3)_2$), 35.7 ($C(CH_3)_2$), 30.9, 27.6 ($OCH(CH_3)_2$), 25.8, 22.3 ($C(CH_3)_2$). Anal. Calcd for $C_{18}H_{25}AlN_4O$: C, 63.51; H, 7.40; N, 16.46. Found: C, 63.89; H, 7.76; N, 16.12.

*Synthesis of [L^{3}AlO^{i}Pr] (***3b***).* 2-Propanol (0.038 g, 0.63 mmol) in 4 mL of toluene was added to a suspension of [L^{3}AlEt] (**3a**) (0.23 g, 0.63 mmol) in 5 mL of a mixed solution of toluene and hexane (1:3 v/v) at room temperature. After the mixture was stirred for 2 h at 70 °C, it was slowly cooled to room temperature overnight. Colorless crystals were obtained that were filtered and washed with hexane. After drying under vacuum for 24 h, an analytically pure product was obtained in 62% yield. The ^{1}H and ^{13}C NMR spectra of **3b** were displayed in Figures S7 and S8 in the Supporting Information. ^{1}H NMR (300 MHz, $CDCl_3$, 25 °C, δ): 7.68 (s, 2H, $N=CH$), 5.82 (s, 2H, pyrrole-*H*), 3.83 (m, 1H, $OCH(CH_3)_2$), 3.46 (d, $J_{H-H} = 12.0$ Hz, 2H, NCH_2), 3.24 (d, $J_{H-H} = 12.0$ Hz, 2H, NCH_2), 2.14 (s, 12H, pyrrole-CH_3), 1.20 (s, 3H, $C(CH_3)_2$), 1.01 (d, 6H, $OCH(CH_3)_2$), 0.96 (s, 3H, $C(CH_3)_2$). ^{13}C NMR (75 MHz, $CDCl_3$, 25 °C, δ): 155.3 ($N=CH$), 148.6, 132.5, 130.8, 115.3 (pyrrole-*C*), 65.5 (NCH_2), 62.5 ($OCH(CH_3)_2$), 35.6 ($C(CH_3)_2$), 28.0, 26.8 ($OCH(CH_3)_2$), 26.6, 26.5 ($C(CH_3)_2$), 15.3 (pyrrole-CH_3), 10.6 (pyrrole-CH_3). Anal. Calcd for $C_{22}H_{33}AlN_4O$: C, 66.64; H, 8.39; N, 14.13. Found: C, 67.25; H, 8.48; N, 13.99.

Lactide Polymerization. In a glovebox, *rac*-LA (1.00 g, 6.94 mmol), 2-propanol (4.33 mg, 0.072 mmol) in 2 mL of toluene, and **1a** (0.020 g, 0.072 mmol) were dissolved in 2 mL of toluene, and another 9 mL of toluene was added successively to a flame-dried reaction vessel equipped with a magnetic stirring bar. The vessel was removed from the glovebox and placed in an oil bath thermostatted at 70 °C. At certain time intervals, an aliquot of the reaction mixture was taken out using a syringe to determine the monomer conversion by ^{1}H NMR. A few drops of acetic acid were added to quench the polymerization after it reached a certain conversion. The polymer was isolated by precipitation in cold methanol, filtered, and dried under vacuum at room temperature for 24 h.

Results and Discussion

Synthesis and Analysis of Complexes. The bis(pyrrolidene) Schiff base ligands H_2L^1, H_2L^2, and H_2L^3 (Scheme 1) were obtained in good yields by reaction of 1,3-propanediamine with pyrrole-2-carboxaldehyde and 2,2-dimethyl-1,3-propanediamine with pyrrole-2-carboxaldehyde or 3,5-dimethylpyrrole-2-carboxaldehyde in absolute methanol at room temperature. Reaction of the ligands H_2L^1, H_2L^2, and H_2L^3 with $AlEt_3$ in anhydrous toluene at 70 °C (Scheme 1) afforded the corresponding aluminum ethyl complexes **1a**, **2a**, and **3a**. The ^{1}H NMR spectrum of compound **2a** (Figure S1 Supporting Information) showed signals at δ −0.15 and 0.82, which are attributed to the methylene protons and methyl protons of the aluminum ethyl group, respectively. In **2a**, the $C(CH_3)_2$ protons display two singlets at 1.06 and 0.89 ppm, and the N=C*H* protons show a singlet at 7.84 ppm. The four NCH_2 protons show two doublets at 3.82 and 3.26 ppm, respectively, which indicates a monomeric structure with a five-coordinated aluminum center. The equal intensities of the signals at 3.82, 3.26, 7.84, and −0.15 ppm confirmed the structure of product **2a**. The geometry of the five-coordinated aluminum complexes is either square pyramidal (sqp) or trigonal bipyramidal (tbp).[22] The symmetric pattern of the pyrrolic protons in the ^{1}H NMR spectrum of **2a** indicates either an exchange between tbp conformations through a sqp transition state on the NMR time scale or a predominantly sqp conformation. Compared with compound **2a**, the signal of the pyrrole-4*H* proton in **3a** has significantly shifted upfield from 6.35 to 5.84 ppm because of the shielding effect of the neighboring methyl groups. The two doublets at 3.54 and 3.24 ppm of the four NCH_2 protons and two singlets at 2.17 and 2.12 ppm for the four methyls on the pyrrolic rings also show a symmetric pattern for **3a** (Figure S5 in the Supporting Information).

The aluminum isopropoxides **2b** and **3b** were obtained by the reaction of the aluminum ethyls **2a** and **3a** with an equimolar amount of 2-propanol in anhydrous toluene at 70 °C (Scheme

Table 1. Polymerization of (*S*,*S*)-LA in Toluene Using Complexes 1a−3a in the Presence of 2-Propanol[a]

entry	complex	M/I	*T* (°C)	time (min)	conv (%)[b]	$M_{n,calcd} \times 10^{3}$[c]	$M_{n,NMR} \times 10^{3}$	$M_{n,GPC} \times 10^{3}$[d]	PDI
1	**1a**	96	70	60	93	12.9	14.1	21.2	1.09
2	**2a**	92	70	180	98	12.9	13.2	19.1	1.10
3	**3a**	96	70	180	96	13.3	13.2	20.1	1.07

[a] All polymerizations were carried out in toluene at 70 °C, $[LA]_0 = 0.474$ mol·L^{-1}. [b] Measured by ^{1}H NMR. [c] Calculated from the equation: $M_{n,calcd} = (M/I) \times conv \times 144$. [d] Determined by GPC in THF, relative to PS standard. The true value of M_n could be calculated according to formula $M_n = 0.58 M_{n,GPC}$.[28]

1). Similar to **2a**, the major peaks in the ^{1}H NMR spectrum of compound **2b** in $CDCl_3$ (Figure S3 in the Supporting Information) show a symmetric pattern with two doublets at 3.88 and 3.23 ppm corresponding to NC*H*$_2$ protons, which indicate a monomeric structure for **2b** with a five-coordinated aluminum center. The appearance of the OCH(CH$_3$)$_2$ methine protons as a multiplet at 3.79 ppm and a doublet of the methyl protons at 1.00 ppm as well as the absence of signals for the aluminum ethyl group showed the complete conversion to the corresponding aluminum isopropoxide complex. However, a minor set of peaks was also observed for **2b** in both $CDCl_3$ and $C_6D_5CD_3$ solutions at room temperature, suggesting the presence of another species that accounts for only 3% in **2b** (Figure S9 in the Supporting Information). It is interesting to note that there exists a slow exchange on the NMR time scale between the two species demonstrated by the presence of positive off-diagonal cross peaks (having phased the diagonal cross peaks in positive sign and the NOE cross-peaks observed at opposite sign) between their NC*H*$_2$ protons in the ^{1}H−^{1}H NOESY NMR spectrum of **2b** (Figure S10 in the Supporting Information). Because the aluminum alkoxides have a tendency to aggregate in solution, a DOSY NMR experiment was carried out using $C_6D_5CD_3$ as the solvent, revealing the same diffusion coefficient for the major and minor species. This suggests that the minor species has an effective hydrodynamic radius that is similar to that of the major species, excluding the formation of dimeric species in the solution. VT ^{1}H NMR experiments were carried out in the range of 295 to 360 K, revealing that the percentage of the minor species increased as the temperature increased (Figure S11 in the Supporting Information). The two minor doublets appearing at 3.18 and 2.43 ppm (295 K) showed no coalescence up to 360 K, indicating that the two Al−N bonds are stable in this minor species. So far, the origin of the formation of the minor species is not clear. However, we propose that compound **2b** mainly adopts a distorted tbp geometry in solution, and the minor species observed for **2b** is probably related to an intermediate species formed in the transformation from one tbp conformational stereoisomer to the other.

(*S*,*S*)-Lactide Polymerization. Polymerizations of (*S*,*S*)-LA in toluene at 70 °C using **1a**, **2a**, and **3a** in the presence of 2-propanol as in situ-forming catalyst/initiator systems were systematically investigated (Table 1). From Table 1, it can be seen that the three complexes **1a**, **2a**, and **3a** are efficient catalysts for the polymerization of (*S*,*S*)-LA. PLAs are obtained with the expected molecular weights and with narrow molecular weight distributions, indicating that the (*S*,*S*)-LA polymerizations initiated by **1a**, **2a**, and **3a** in the presence of 2-propanol were living. The polymerization of ca. 100 equiv of (*S*,*S*)-LA goes to completion within 60 min (93% conversion) at 70 °C applying **1a**/2-propanol. However, this period is prolonged to 180 min when the **2a**/2-propanol (98% conversion) or **3a**/2-propanol (96% conversion) system is used. Nonligated metal alkoxides usually give epimerization of LA monomer, PLAs, or both when applied in (*S*,*S*)-LA polymerization.[4c,23] Therefore, (*S*,*S*)-LA polymerization was performed under similar conditions using **2a**/2-propanol as the catalyst/initiator system. The appearance of only one single peak of a *mmmmm* hextrad in the methine carbon region in the ^{13}C NMR spectrum (Figure S12 in Supporting Information) revealed that in the presence of 2-propanol complex **2a** afforded a highly isotactic PLLA material without significant epimerization of either the monomer or the resulting polymer.

Scheme 2. Stereochemistry of *rac*- and *meso*-LA polymerization by Using (In Situ-Forming) Bis(Pyrrolidene) Schiff Base Aluminum Isopropoxide System[a]

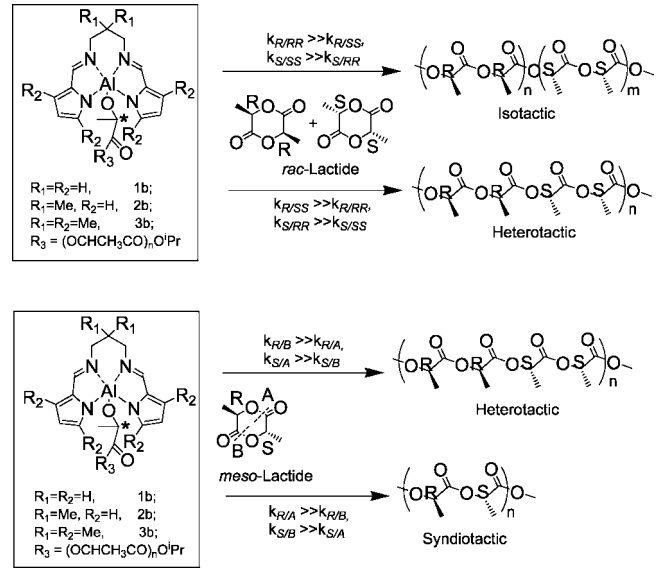

[a] * represents the R stereogenic center in the last unit along the propagating chain.

Stereochemistry of Lactide Polymerization. The stereochemical microstructures of the isolated PLAs were determined from the methine region of the homonuclear decoupled ^{1}H NMR spectra. Because all bis(pyrrolidene) Schiff base ligands prepared were achiral, it was anticipated that stereoselectivity in the polymerization of *rac*- and *meso*-LA by this achiral catalyst/initiator system takes place via the chain-end control mechanism. In such a reaction, the configuration of the inserted monomer in *rac*-LA polymerization or the cleavage site of the monomer in *meso*-LA polymerization is determined by the stereogenic center of the last lactic acid unit along the propagating chain. If the stereogenic center in the last repeating unit favors a *meso*-enchainment, which means a chain end of R stereochemistry selects (*R*,*R*)-LA in *rac*-LA or selects the B site to cleave *meso*-LA, then isotactic PLA is obtained from *rac*-LA ($k_{R/RR} \gg k_{R/SS}$) and heterotactic PLA will be obtained by using *meso*-LA ($k_{R/B} \gg k_{R/A}$). However, if the stereogenic center in the last repeating unit favors a racemic enchainment, which means a chain end of R stereochemistry selects (*S*,*S*)-LA in *rac*-LA or selects the A site to cleave *meso*-LA, then hetereotactic PLA will be obtained from *rac*-LA ($k_{R/SS} \gg k_{R/RR}$) and syndiotactic PLA will be obtained from *meso*-LA ($k_{R/A} \gg k_{R/B}$) (Scheme 2).

The PLA material produced by **2a**/2-propanol in the ring-opening polymerization of *rac*-LA at 70 °C in toluene is substantially isotactic with a P_m of 0.74 (Table 2, entries 2−5). The methine region of the homonuclear decoupled ^{1}H NMR spectrum is depicted in Figure 1a. Increasing the temperature

Table 2. Polymerization of *rac*-LA in Toluene Using Complexes 1a−3a in the Presence of 2-Propanol, 2b, and 3b[a]

entry	complex	M/I	T (°C)	time (min)	conv (%)[b]	$M_{n,calcd} \times 10^{3}$[c]	$M_{n,NMR} \times 10^{3}$	$M_{n,GPC} \times 10^{3}$[d]	P_m[e]	PDI
1	**1a**	96	70	60	93.0	12.9	11.2	26.6	0.65	1.10
2	**2a**	48	70	150	>99.0	6.85	7.69	15.2	0.74	1.20
3	**2a**	72	70	150	98.0	10.2	11.5	21.7	0.74	1.11
4	**2a**	84	70	150	88.5	10.8	10.6	25.7	0.74	1.07
5	**2a**	96	70	150	74.6	10.4	10.5	26.0	0.74	1.07
6	**2a**	96	90	90	94.6	13.1	12.3	26.7	0.72	1.13
7	**2a**	96	110	60	92.0	12.7	9.76	26.7	0.68	1.24
8	**2b**	96	70	90	96.2	13.3	14.6	32.9	0.75	1.24
9	**3a**	96	70	240	96.4	13.3	13.1	26.6	0.60	1.04
10	**3b**	96	70	120	87.6	12.1	10.8	20.0	0.62	1.05

[a] All polymerizations were carried out in toluene at 70 °C, $[LA]_0 = 0.474$ mol·L^{-1}. [b] Measured by ^{1}H NMR. [c] Calculated from the equation: $M_{n,calcd} = (M/I) \times conv \times 144$. [d] Determined by GPC in THF, relative to PS standard. The true value of M_n could be calculated according to formula $M_n = 0.58M_{n,GPC}$.[28] [e] Parameter P_m is the probability to give *meso* enchainment between monomer units and is determined from the methine region of the homonuclear decoupled ^{1}H NMR spectrum.

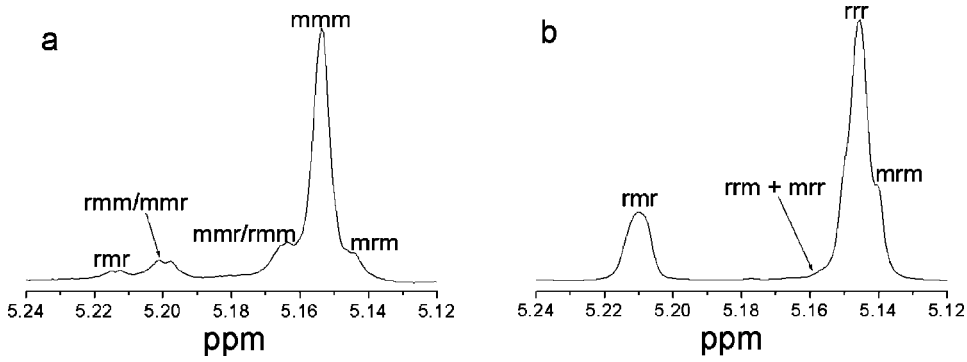

Figure 1. Methine region of homonuclear decoupled ^{1}H NMR spectra of isolated PLA materials: (a) from *rac*-LA using **2a**/2-propanol; (b) from *meso*-LA using **1a**/2-propanol.

Table 3. Polymerization of *meso*-LA in Toluene Using Complexes 1a−3a in the Presence of 2-Propanol[a]

entry	complex	M/I	T (°C)	time (min)	conv (%)[b]	$M_{n,calcd} \times 10^{3}$[c]	$M_{n,NMR} \times 10^{3}$	$M_{n,GPC} \times 10^{3}$[d]	P_r[e]	PDI
1	**1a**	96	70	90	93	12.9	13.3	24.1	0.56	1.16
2	**2a**	96	70	150	47	6.50	6.72	10.4	0.57	1.12
3	**3a**	96	70	240	94	13.0	10.4	18.6	0.53	1.06

[a] All polymerizations were carried out in toluene solution at 70 °C, $[LA]_0 = 0.474$ mol·L^{-1}. [b] Measured by ^{1}H NMR. [c] Calculated from the equation: $M_{n,calcd} = (M/I) \times conv \times 144$. [d] Determined by GPC in THF, relative to PS standard. The true value of M_n could be calculated according to formula $M_n = 0.58M_{n,GPC}$.[28] [e] Parameter P_r is the probability to give racemic enchainment between monomer units and is determined from the methine region of the homonuclear decoupled ^{1}H NMR spectrum.

of the reaction mixture to either 90 or 110 °C results in a decrease in the P_m of the resulting polymer to, respectively, 0.72 and 0.68 (Table 2, entries 6 and 7).

According to first-order Markovian statistics[24] and absolute reaction rate theory, eq 1 can be used to determine the activation entropy difference ($\Delta S_m^{\ddagger} - \Delta S_r^{\ddagger}$) and activation enthalpy difference ($\Delta H_m^{\ddagger} - \Delta H_r^{\ddagger}$) between homopropagation (k_m) and cross-propagation (k_r).

$$P_m/(1 - P_m) = k_m/k_r = \exp\left[(\Delta S_m^{\ddagger} - \Delta S_r^{\ddagger})/R - (\Delta H_m^{\ddagger} - \Delta H_r^{\ddagger})/RT\right] \quad (1)$$

$\ln[P_m/(1 - P_m)]$ was plotted against $10^3/T$ (Figure S13 in Supporting Information). From this plot, an activation entropy difference ($\Delta S_m^{\ddagger} - \Delta S_r^{\ddagger}$) of −14.27 cal·K^{-1}·mol^{-1} and an activation enthalpy difference ($\Delta H_m^{\ddagger} - \Delta H_r^{\ddagger}$) of −7.93 kcal·mol^{-1} were found, showing the preference of isotactic enchainment. Furthermore, the polymerization data indicate that the introduction of methyl groups to the auxiliary ligand significantly affects the stereoselectivity. For instance, polymerization of *rac*-LA using **1a**/2-propanol furnished an isotactic-biased material with a P_m of 0.65 (Table 2, entry 1), which is lower than that of **2a**/2-propanol ($P_m = 0.74$), indicating that the presence of the gem methyls on the propylene diimine bridge remarkably enhances the stereoselectivity, which is consistent with a previous study.[21b] However, it is interesting to note that the catalyst/initiator system **3a**/2-propanol affords PLA material from *rac*-LA with a lower P_m value of 0.60 (Table 2, entry 9) compared with the PLA formed by **2a**/2-propanol ($P_m = 0.74$), revealing that the enhanced chain-end control in the polymerization by the methyl substituents on pyrrolic rings leads to an increased heterotactic enchainment. A similar effect has been once reported by Gibson for a bis(salicylidene) Schiff base aluminum complex with a rigid diarylene diimine bridge.[21a] Polymerizations of *meso*-LA with **1a**, **2a**, and **3a** in the presence of 2-propanol all furnish nearly atactic polymers with P_r values of 0.56 (Figure 1b), 0.57, and 0.53 (Table 3), respectively. The minor difference in the tacticities of these polymers also reveals that the substituent on the ligand hardly influences the chain-end control ability toward *meso*-LA polymerization.

The putative active species formed upon reaction of the bis(pyrrolidene) Schiff base aluminum ethyls with 2-propanol are the corresponding aluminum ispropoxides. Therefore, the bis(pyrrolidene) Schiff base aluminum isopropoxide **2b** and **3b** were prepared. The synthesis of PLAs by the ring-opening polymerization of *rac*-LA using **2b** and **3b** allowed a comparison between the behavior of aluminum isopropoxides and the compounds formed by the in situ reaction between the aluminum ethyl compounds and 2-propanol. The PLA obtained by the ring-opening polymerization of *rac*-LA using **2b** has approximately the same P_m value of 0.75 (Table 2, entry 8) as the polymer obtained via **2a**/2-propanol ($P_m = 0.74$). Similarly, compound **3b** furnished PLA with a P_m of 0.62 (Table 2, entry 10), which

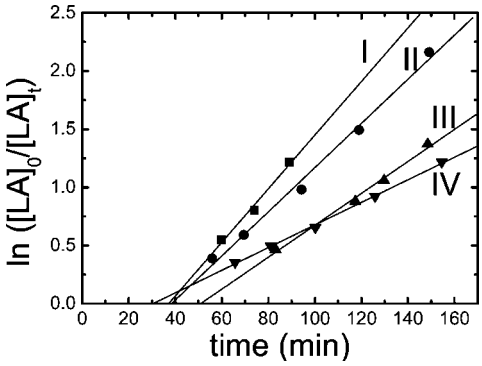

Figure 2. First-order kinetics plots for the polymerization of *rac*-LA by applying **2a**/2-propanol as catalyst/initiator in toluene at 70 °C with $[LA]_0 = 0.534$ mol·L^{-1}: (I) $[Al]_0 = 7.42 \times 10^{-3}$ mol·L^{-1}, $k_{app} = 23.1 \times 10^{-3}$ min^{-1}; (II) $[Al]_0 = 6.36 \times 10^{-3}$ mol·L^{-1}, $k_{app} = 19.0 \times 10^{-3}$ min^{-1}; with $[LA]_0 = 0.474$ mol·L^{-1}: (III) $[Al]_0 = 4.94 \times 10^{-3}$ mol·L^{-1}, $k_{app} = 13.7 \times 10^{-3}$ min^{-1}; and with $[LA]_0 = 0.237$ mol·L^{-1}: (IV) $[Al]_0 = 3.55 \times 10^{-3}$ mol·L^{-1}, $k_{app} = 9.72 \times 10^{-3}$ min^{-1}.

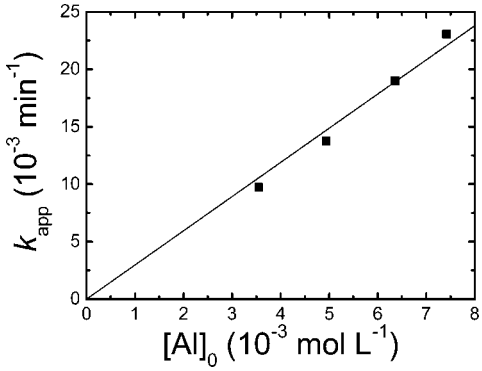

Figure 3. Linear plot of k_{app} versus $[Al]_0$ for the polymerization of *rac*-LA using **2a**/2-propanol as catalyst/initiator (toluene, 70 °C, $k_p = 2.97$ L·mol^{-1}·min^{-1}, $R^2 = 0.996$).

is close to that of **3a**/2-propanol ($P_m = 0.60$). Moreover, the *N*,*N*,*N*,*N*-tetradentate coordination mode of the bis(pyrrolidene) Schiff base ligand in **2b** caused an isoselectivity enhancement ($P_m = 0.75$) in *rac*-LA polymerization compared with that of *N*,*N*′-(2,2-dimethyl-1,3-propylene) bis(salicylideneiminato) aluminum ethyl in the presence of 2-propanol ($P_m = 0.67$), which has a *N*,*N*,*O*,*O*-tetradentate coordination mode of the bis(salicylidene) Schiff base ligand.[21b] ^{1}H NMR spectra revealed the presence of aggregated species of the *N*,*N*′-(2,2-dimethyl-1,3-propylene) bis(salicylideneiminato) aluminum isopropoxide, which is not the case for **2b** in solution. The isoselectivity enhancement for **2b** is most probably due to the presence of only a monomeric species in solution.

Mechanism and Kinetics of Lactide Polymerization. The ^{1}H NMR spectrum of PLA oligomers prepared using **2a**/2-propanol at a low monomer-to-initiator ratio of 13 showed a triplet of two overlapping doublets at 1.24 ppm and a quartet at 4.34 ppm with an integral ratio close to 6:1. These peaks were assigned to the methyl protons of the isopropoxycarbonyl end group and the methine proton neighboring the hydroxyl end group, respectively. This clearly indicates that the oligomer is systematically capped with one isopropyl ester group and one hydroxyl group. This confirms that the aluminum isopropoxides were the actual active species in LA polymerizations when applying aluminum ethyls/2-propanol as catalyst/initiator systems. The M_n of the oligomer determined by end-group analysis is 1760, which is close to the theoretical value of 1500.

The kinetics of the ring-opening polymerization of *rac*-LA ($[LA]_0 = 0.534$, 0.474, and 0.237 mol·L^{-1}) at various concentrations of **2a** ((3.55 to 7.42) $\times 10^{-3}$ mol·L^{-1}) in the presence of 2-propanol in toluene at 70 °C were monitored by ^{1}H NMR spectroscopy until all monomer was consumed. Semilogarithmic plots for these polymerizations are shown in Figure 2. In each case, an induction period and first-order kinetics in monomer were observed. The induction period implies that complex **2a** reacted with 2-propanol to form the aluminum isopropoxide as the actual active species to initiate the polymerizations. Thus, the polymerization of *rac*-LA by using **2a**/2-propanol proceeds according to

$$-\mathrm{d}[LA]/\mathrm{d}t = k_{app}[LA] \quad (2)$$

where $k_{app} = k_p[Al]^x$, and k_p is the polymerization rate constant. The linear relationship of k_{app} versus $[Al]_0$ reveals a first-order in catalyst (Figure 3). Therefore, the polymerization of *rac*-LA initiated and catalyzed by **2a**/2-propanol follows an overall kinetics law of the following form

$$-\mathrm{d}[LA]/\mathrm{d}t = k_p[Al][LA] \quad (3)$$

A k_p value of 2.97 L·mol^{-1}·min^{-1} was determined (Table 4, entry 3) for **2a**/2-propanol in toluene at 70 °C. This value is significantly lower than that determined for (*S*,*S*)-LA polymerization (4.83 L·mol^{-1}·min^{-1}) and much higher than that determined for *meso*-LA polymerization (0.93 L·mol^{-1}·min^{-1}) (Figure 4). Predominant formation of isotactic structures from *rac*-LA polymerization means a significantly higher rate of homopropagation ($k_{R/RR}$ or $k_{S/SS}$) than cross propagation ($k_{R/SS}$ or $k_{S/RR}$). The significantly faster polymerization of (*S*,*S*)-LA compared with that of *rac*-LA is consistent with this observation.

Conversions versus time data were also collected for the polymerization of *rac*- and *meso*-LA with **1a** and **3a** in the presence of 2-propanol (toluene; 70 °C; $[LA]_0 = 0.474$ mol·L^{-1};

Table 4. Kinetic Results of *rac*- and *meso*-LA Polymerization Using Complexes 1a−3a in the Presence of 2-Propanol, 2b, and 3b[a]

entry	complex	monomer	$k_{app} \times 10^{-3}$ min^{-1}[b]	k_p L·mol^{-1}·min^{-1}[c]
1	**1a**	*rac*-LA	38.5	7.79
2	**1a**	*meso*-LA	29.4	5.95
3	**2a**	*rac*-LA	13.7	2.97[d]
4	**2a**	*meso*-LA	4.60	0.93
5	**2b**	*rac*-LA	55.3	13.0[d]
6	**3a**	*rac*-LA	17.0	3.44
7	**3a**	*meso*-LA	13.5	2.73
8	**3b**	*rac*-LA	17.1	3.46

[a] Studies of kinetics were carried out at 70 °C using toluene as a solvent, $[LA]_0 = 0.474$ mol·L^{-1}, $[Al]_0 = 4.94 \times 10^{-3}$ mol·L^{-1}. [b] Measured by ^{1}H NMR. [c] Calculated from the relationship: $k_p = k_{app}/[Al]_0$. [d] Deduced from the linear plot of k_p against $[Al]_0$.

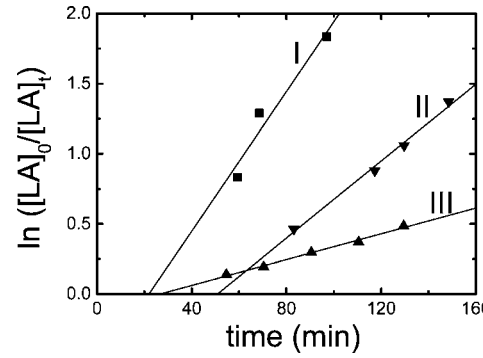

Figure 4. First-order kinetics plots for the polymerization of (*S*,*S*)-, *rac*-, and *meso*-LA by using **2a**/2-propanol as catalyst/initiator in toluene at 70 °C with $[LA]_0 = 0.474$ mol·L^{-1}: (I) (*S*,*S*)-LA, $[Al]_0 = 5.15 \times 10^{-3}$ mol·L^{-1}, $k_{app} = 24.9 \times 10^{-3}$ min^{-1}; (II) *rac*-LA, $[Al]_0 = 4.94 \times 10^{-3}$ mol·L^{-1}, $k_{app} = 13.7 \times 10^{-3}$ min^{-1}; (III) *meso*-LA, $[Al]_0 = 4.94 \times 10^{-3}$ mol·L^{-1}, $k_{app} = 4.60 \times 10^{-3}$ min^{-1}.

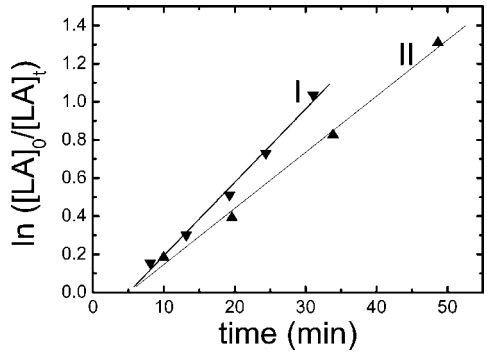

Figure 5. First-order kinetics plots for the polymerization of *rac*- and *meso*-LA by using **1a**/2-propanol as catalyst/initiator in toluene at 70 °C with $[LA]_0 = 0.474$ mol·L^{-1}, $[Al]_0 = 4.94 \times 10^{-3}$ mol·L^{-1}: (I) *rac*-LA, $k_{app} = 38.5 \times 10^{-3}$ min^{-1}; (II) *meso*-LA, $k_{app} = 29.4 \times 10^{-3}$ min^{-1}.

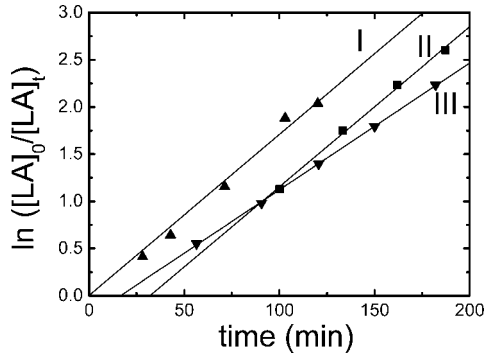

Figure 6. First-order kinetics plots for the polymerization of *rac*-LA by using **3a**/2-propanol as catalyst/initiator and **3b** in toluene at 70 °C with $[LA]_0 = 0.474$ mol·L^{-1}, $[Al]_0 = 4.94 \times 10^{-3}$ mol·L^{-1}: (I) **3b**, $k_{app} = 17.1 \times 10^{-3}$ min^{-1}; (II) **3a**, $k_{app} = 17.0 \times 10^{-3}$ min^{-1}. First-order kinetics plots for the polymerization of *meso*-LA by using complex **3a**/2-propanol as catalyst/initiator in toluene at 70 °C with $[LA]_0 = 0.474$ mol·L^{-1}, $[Al]_0 = 4.94 \times 10^{-3}$ mol·L^{-1}: (III) **3a**, $k_{app} = 13.5 \times 10^{-3}$ min^{-1}.

$[Al]_0 = 4.94 \times 10^{-3}$ mol·L^{-1}). In each case, first-order kinetics in monomer was observed. The semilogarithmic plots for polymerizations using **1a**/2-propanol are shown in Figure 5, and those for **3a**/2-propanol are depicted in Figure 6. The corresponding k_p values were deduced according to the relationship $k_p = k_{app}/[Al]_0$ and are listed in Table 4. The polymerization rate for *meso*-LA polymerization ($k_p = 5.95$ L·mol^{-1}·min^{-1}) is slightly lower than that for *rac*-LA polymerization ($k_p = 7.97$ L·mol^{-1}·min^{-1}) using **1a**/2-propanol. In the polymerization applying **3a**/2-propanol, the polymerization rate for *meso*-LA polymerization ($k_p = 2.73$ L·mol^{-1}·min^{-1}) is also slightly lower than that for *rac*-LA polymerization ($k_p = 3.44$ L·mol^{-1}·min^{-1}). Consistent valence force field (CVFF) calculations revealed that *meso*-LA monomer is less stable in the ground state than are (*S*,*S*)- and *rac*-LA.[25] This may imply that *meso*-LA will be more easily cleaved than *rac*-LA monomer when coordinated to the metal center, which will lead to a higher polymerization rate for *meso*-LA than for *rac*-LA. Therefore, it is apparent that the low activity for *meso*-LA polymerization by using the bis(pyrrolidene) Schiff base aluminum systems is mainly due to the chain-end selection effect caused by the presence of both R- and S-stereogenic centers in the last repeating unit along the propagation chain.

The influence of the temperature on the polymerization rate of *rac*-LA using **2a**/2-propanol was also investigated. As depicted in Figure 7, the polymerization rate increased with increasing temperature. The values of k_{app} were 31.9×10^{-3} min^{-1} at 90 °C and 53.7×10^{-3} min^{-1} at 110 °C, respectively.

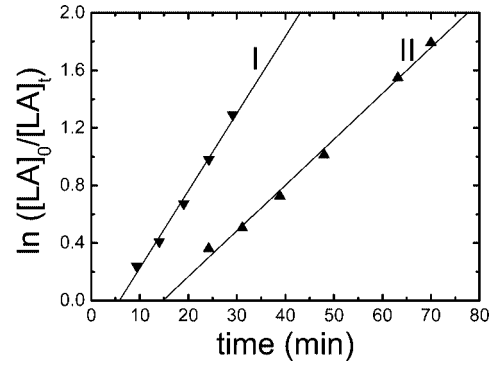

Figure 7. First-order kinetics plots for the polymerization of *rac*-LA by using **2a**/2-propanol as catalyst/initiator in toluene at 90 and 110 °C with $[LA]_0 = 0.474$ mol·L^{-1}: (I) 110 °C, $[Al]_0 = 4.94 \times 10^{-3}$ mol·L^{-1}, $k_{app} = 53.7 \times 10^{-3}$ min^{-1}; (II) 90 °C, $[Al]_0 = 4.94 \times 10^{-3}$ mol·L^{-1}, $k_{app} = 31.9 \times 10^{-3}$ min^{-1}.

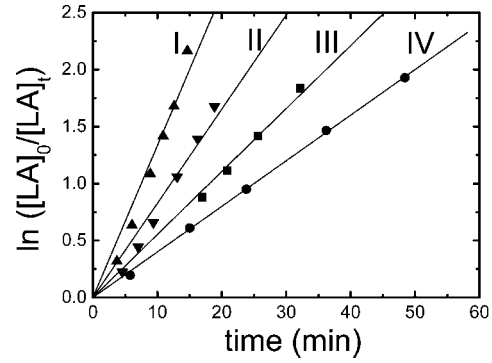

Figure 8. First-order kinetics plots for the polymerization of *rac*-LA by complex **2b** in toluene at 70 °C with $[LA]_0 = 0.474$ mol·L^{-1}: (I) $[Al]_0 = 9.88 \times 10^{-3}$ mol·L^{-1}, $k_{app} = 133 \times 10^{-3}$ min^{-1}; (II) $[Al]_0 = 6.58 \times 10^{-3}$ mol·L^{-1}, $k_{app} = 82.6 \times 10^{-3}$ min^{-1}; (III) $[Al]_0 = 4.94 \times 10^{-3}$ mol·L^{-1}, $k_{app} = 55.3 \times 10^{-3}$ min^{-1}; and with $[LA]_0 = 0.237$ mol·L^{-1}: (IV) $[Al]_0 = 2.47 \times 10^{-3}$ mol·L^{-1}, $k_{app} = 40.0 \times 10^{-3}$ min^{-1}.

According to the relationship $k_p = k_{app}/[Al]_0$, the values of k_p at 90 and 110 °C were calculated to be 6.46 and 10.9 L·mol^{-1}·min^{-1}, respectively. From the three k_p values determined at different temperatures, the activation energy of the polymerization using **2a**/2-propanol was deduced by fitting ln k_p versus $10^3/T$ according to the Arrhenius equation (Figure S14 in Supporting Information). The activation energy E_a for the *rac*-LA polymerization using **2a**/2-propanol was 35.5 kJ·mol^{-1}, which is comparable to that for the ring-opening polymerization of (*S*,*S*)-LA initiated by aluminum trialkoxides functionalized with (2-methacryloxy)ethyloxy (35.5 kJ·mol^{-1})[26] but is much lower than that of (*S*,*S*)-LA polymerization initiated by tin octanoate (70.9 kJ·mol^{-1}).[27]

Aluminum isopropoxides **2b** and **3b**, which were considered to be the initiating species, were subsequently investigated toward their reactivities in *rac*-LA polymerization. Interestingly, the single-site aluminum isopropoxide **2b** exhibits a much higher activity compared with the in situ-formed aluminum isopropoxide from **2a**/2-propanol. In each case, a first-order kinetics in monomer was observed, and the appropriate semilogarithmic plots ($[LA]_0 = 0.474$ mol·L^{-1}, $[Al]_0 = (2.47$ to $9.88) \times 10^{-3}$ mol·L^{-1}) for these polymerizations are shown in Figure 8. No significant induction period was observed in each case, which indicates that the aluminum isopropoxide **2b** acts as the actual active species in the ring-opening polymerization of LA. The linear relationship between k_{app} versus $[Al]_0$, as depicted in Figure 9, revealed that the polymerization using **2b** is also first-order in both monomer and catalyst. The k_p value for polym-

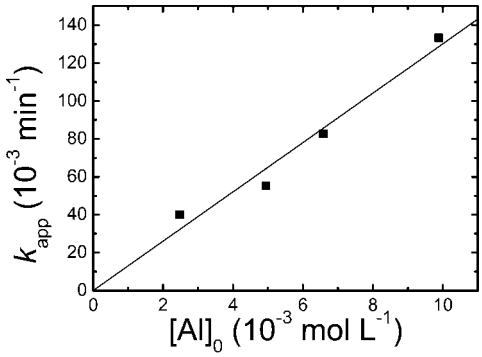

Figure 9. Linear plot of k_{app} versus $[Al]_0$ for the polymerization of *rac*-LA with complex **2b** (toluene, 70 °C, $k_p = 13.0$ L·mol^{-1}·min^{-1}, $R^2 = 0.966$).

erization of *rac*-LA using **2b** was calculated to be 13.0 L·mol^{-1}·min^{-1}, which is even comparable to those of bis(salicylidene) Schiff base aluminum initiators with chlorine atoms at the ortho and para positions of the phenol group[21a,b] and is much higher than those of aluminum initiators comprising nonsubstituted or *tert*-butyl-substituted bis(salicylidene) Schiff base ligands.[19a] The k_p value for polymerization of *rac*-LA using **2b** is almost three times higher than that of **2a**/2-propanol ($k_p = 2.97$ L·mol^{-1}·min^{-1}). For polymerizations using in situ alcoholysis of aluminum ethyls, the polymerization consists of two steps. In the first step, the aluminum ethyls react with 2-propanol with a rate constant k_{rea} to produce the aluminum isopropoxide as the active species. Consecutively, the aluminum isopropoxide initiates the LA polymerization with a polymerization rate constant k_p immediately after it is generated and until equilibrium of monomer conversion is reached. If $k_{rea} \gg k_p$, then the observed polymerization rate is mainly determined by and presumably equal to k_p. However, if $k_{rea} \leq k_p$, then the observed polymerization rate will be influenced by k_{rea}. We assume that for **2a**/2-propanol, the k_p is much higher than the k_{rea}, which causes the lower observed polymerization rate (2.97 L·mol^{-1}·min^{-1}) for *rac*-LA polymerization using **2a**/2-propanol compared with the polymerization rate (13.0 L·mol^{-1}·min^{-1}) for **2b**. On the basis of the narrow molecular weight distributions (Table 2, entries 2−7) observed and the fact that the number-average molecular weights of the isolated PLAs initiated by **2a**/2-propanol are in good accordance with the calculated ones, this indicates that fast chain transfer is taking place during polymerization. However, according to the kinetics data, it is apparent that the polymerizations of *rac*-LA using **3a**/2-propanol or **3b** have almost similar polymerization rates ($k_p = 3.44$ L·mol^{-1}·min^{-1} for **3a**/2-propanol compared with $k_p = 3.46$ L·mol^{-1}·min^{-1} for **3b**). Thus, it is envisioned that for the polymerization initiated by **3a**/2-propanol, k_p is much lower than k_{rea}. The k_p value for **3b** is lower than that of **2b**, indicating that the presence of the methyl substituents at the ortho position of the pyrrolic rings retard the polymerization process. Although the *rac*-LA polymerization using the aluminum isopropoxide formed by **1a** and 2-propanol has not been carried out, we assume that **1a**/2-propanol has a much higher k_{rea} than k_p, which leads to no significant differences in k_p for **1a**/2-propanol ($k_p = 7.79$ L·mol^{-1}·min^{-1}) and its aluminum isopropoxide. From the comparison of **1a**/2-propanol and **2b**, it is clear that the gem methyls on the propylene backbones greatly enhance the rate of polymerization, which is consistent with our previous report.[21b]

Conclusions

We report a series of aluminum ethyl and isopropoxide complexes ligated by *N*,*N*,*N*,*N*-tetradentate bis(pyrrolidene) Schiff base ligands that act as single-site catalysts for the polymerization of (*S*,*S*)-LA to isotactic PLA, *rac*-LA to predominant isotactic PLA, and *meso*-LA to atactic PLA. The study of kinetics indicates that the activity of the bis(pyrrolidene) Schiff base aluminum initiator system toward LA polymerization decreases in the order of (*S*,*S*)-lactide > *rac*-lactide > *meso*-lactide, which is consistent with the observed isotacticity for the resulting PLAs prepared from *rac*-LA. The low stereoselectivity and low activity of the bis(pyrrolidene) Schiff base aluminum initiators in *meso*-LA polymerization compared with *rac*-LA polymerization reflect the chain-end selection effect by first-order Markovian statistics caused by the presence of both R- and S-stereogenic centers in the last repeating unit along the propagating chain. Microstructural analysis of the polymers formed as well as kinetics data show that the gem methyls on the diimine bridge enhance not only the isoselectivity but also the polymerization rate of **2a**/2-propanol or **2b**. However, the methyl substituents at the ortho position of the pyrrolic rings both decrease the polymerization rate and the isoselectivity of **3a**/2-propanol or **3b**. Furthermore, the analysis of the kinetics reveals that the polymerizations of *rac*-LA using **2a**/2-propanol or **2b** are first-order with respect to both monomer and catalyst. Finally, a comparison of k_p values reveals that the polymerization rate of **2b** is higher than that of **2a**/2-propanol.

Acknowledgment. We thank the Chinese Academy of Sciences and the Royal Netherlands Academy of Arts and Sciences for the CAS-KNAW joint training Ph.D. program (06PhD09). A.H.V acknowledges the Dutch nanotechnology program NanoNed for financial support.

Supporting Information Available: ^{1}H and ^{13}C NMR spectra of complexes **2a**, **3a**, **2b**, and **3b**, ^{1}H−^{1}H NOESY and VT ^{1}H NMR spectrum of **2b**, and kinetics figures. This material is available free of charge via the Internet at http://pubs.acs.org.

References and Notes

(1) (a) Ikada, Y.; Tsuji, H. *Macromol. Rapid Commun.* **2000**, *21*, 117–132. (b) Winzenburg, G.; Schmidt, C.; Fuchs, S.; Kissel, T. *Adv. Drug Delivery Rev.* **2004**, *56*, 1453–1466. (c) Auras, R.; Harte, B.; Selke, S. *Macromol. Biosci.* **2004**, *4*, 835–864. (d) Guarino, V.; Causa, F.; Taddei, P.; di Foggia, M.; Ciapetti, G.; Martini, D.; Fagnano, C.; Baldini, N.; Ambrosio, L. *Biomaterials* **2008**, *29*, 3662–3670.
(2) (a) Dubois, Ph; Jacobs, C.; Jerome, R.; Teyssie, Ph *Macromolecules* **1991**, *24*, 2266–2270. (b) Kowalski, A.; Duda, A.; Penczek, S. *Macromolecules* **1998**, *31*, 2114–2122.
(3) Kricheldorf, H. R.; Boettcher, C. *Makromol. Chem.* **1993**, *194*, 1665–1669.
(4) (a) Zhong, Z.; Dijkstra, P. J.; Birg, C.; Westerhausen, M.; Feijen, J. *Macromolecules* **2001**, *34*, 3863–3868. (b) Zhong, Z.; Schneiderbauer, S.; Dijkstra, P. J.; Westerhausen, M.; Feijen, J. *J. Polym. Environ.* **2001**, *9*, 31–38. (c) Zhong, Z.; Ankone, M.J. K.; Dijkstra, P. J.; Birg, C.; Westerhausen, M.; Feijen, J. *Polym. Bull* **2001**, *46*, 51–57.
(5) (a) O'Keefe, B. J.; Monnier, S. M.; Hillmyer, M. A.; Tolman, W. B. *J. Am. Chem. Soc.* **2001**, *123*, 339–340. (b) O'Keefe, B. J.; Breyfogle, L. E.; Hillmyer, M. A.; Tolman, W. B. *J. Am. Chem. Soc.* **2002**, *124*, 4384–4393. (c) Wang, X.; Liao, K.; Quan, D.; Wu, Q. *Macromolecules* **2005**, *38*, 4611–4617.
(6) (a) Kowalski, A.; Libiszowski, J.; Duda, A.; Penczek, S. *Macromolecules* **2000**, *33*, 1964–1971. (b) Duda, A.; Penczek, S.; Kowalski, A. *Macromol. Symp.* **2000**, *153*, 41–53.
(7) Schwach, G.; Coudane, J.; Engel, R.; Vert, M. *Polym. Int.* **1998**, *46*, 177–182.
(8) (a) Stevels, W. M.; Ankone, M. J. K.; Dijkstra, P. J.; Feijen, J. *Macromolecules* **1996**, *29*, 3332–3333. (b) Stevels, W. M.; Ankone, M. J. K.; Dijkstra, P. J.; Feijen, J. *Macromolecules* **1996**, *29*, 6132–6138. (c) Simic, V.; Spassky, N.; Hubert-Pfalzgraf, L. G. *Macromolecules* **1997**, *30*, 7338–7340. (d) Zhang, L.; Sheng, Z.; Yu, C.; Fan, L. *J. Mol. Catal. A: Chem.* **2004**, *214*, 199–202.
(9) (a) Spassky, N.; Simic, V.; Montaudo, M. S.; Hubert-Pfalzgraf, L. G. *Macromol. Chem. Phys.* **2000**, *201*, 2432–2440. (b) Chisholm, M. H.; Delbridge, E. E.; Gallucci, J. C. *New. J. Chem.* **2004**, *1*, 145–152.
(10) Coates, G. W. *Chem. Rev.* **2000**, *100*, 1223–1252.

(11) For recent reviews on lactide polymerization using single-site metal catalysts, see: (a) O'Keefe, B.; Hillmyer, M.; Tolman, W. B.*J. Chem. Soc., Dalton Trans.* **2001**, *15*, 2215–2224. (b) Coates, G. W. *J. Chem. Soc., Dalton Trans.* **2002**, *4*, 467–475. (c) Dechy-Cabaret, O.; Martin-Vaca, B.; Bourissou, D. *Chem. Rev.* **2004**, *104*, 6147–6176. (d) Wu, J.; Yu, T.-L.; Chen, C.-T.; Lin, C.-C. *Coord. Chem. Rev.* **2006**, *250*, 602–626. (e) Platel, R. H.; Hodgson, L. M.; Williams, C. K. *Polym. Rev.* **2008**, *48*, 11–63.

(12) (a) Cheng, M.; Attygalle, A.; Lobkovsky, E.; Coates, G. W. *J. Am. Chem. Soc.* **1999**, *121*, 11583–11584. (b) Chamberlain, B.; Cheng, M.; Moore, D.; Ovitt, T.; Lobkovsky, E.; Coates, G. W. *J. Am. Chem. Soc.* **2001**, *123*, 3229–3238. (c) Chen, H.-Y.; Huang, B.-H.; Lin, C.-C. *Macromolecules* **2005**, *38*, 5400–5405.

(13) (a) Chisholm, M. H.; Huffman, J. C.; Phomphrai, K. *J. Chem. Soc., Dalton Trans.* **2001**, *3*, 222–224. (b) Chisholm, M. H.; Gallucci, J.; Phomphrai, K. *Inorg. Chem.* **2002**, *41*, 2785–2794. (c) Dove, A. P.; Gibson, V. C.; Marshall, E. L.; White, A. J. P.; Williams, D. J. *J. Chem. Soc., Dalton Trans.* **2004**, *4*, 570–578.

(14) Bouyahyi, M.; Grunova, E.; Marquet, N.; Kirillov, E.; Thomas, C. M.; Roisnel, T.; Carpentier, J.-F. *Organometallics* **2008**, *27*, 5815–5825.

(15) Chmura, A. J.; Chuck, C. J.; Davidson, M. G.; Jones, M. D.; Lunn, M. D.; Bull, S. D.; Mahon, M. F. *Angew. Chem., Int. Ed.* **2007**, *46*, 2280–2283.

(16) (a) Chmura, A. J.; Davidson, M. G.; Frankis, C. J.; Jones, M. D.; Lunn, M. D. *Chem. Commun.* **2008**, *11*, 1293–1295. (b) Chmura, A. J.; Davidson, M. G.; Jones, M. D.; Lunn, M. D.; Mathon, M. F.; Johnson, A. F.; Khunkamchoo, P.; Roberts, S. L.; Wong, S. S. F. *Macromolecules* **2006**, *39*, 7250–7257. (c) Gendler, S.; Segal, S.; Goldberg, I.; Goldschmidt, Z.; Kol, M. *Inorg. Chem.* **2006**, *45*, 4783–4790.

(17) (a) Ma, H.; Spaniol, T. P.; Okuda, J. *J. Chem. Soc., Dalton Trans.* **2003**, *24*, 4770–4780. (b) Cai, C.-X.; Amgoune, A.; Lehmann, C. W.; Carpentier, J.-F. *Chem. Commun.* **2004**, *3*, 330–331. (c) Ma, H.; Okuda, J. *Macromolecules* **2005**, *38*, 2665–2673. (d) Bonnet, F.; Cowley, A. R.; Mountford, P. *Inorg. Chem.* **2005**, *44*, 9046–9055. (e) Amgoune, A.; Thomas, C. M.; Roisnel, T.; Carpentier, J.-F. *Chem.—Eur. J.* **2006**, *12*, 169–179. (f) Ma, H.; Spaniol, T. P.; Okuda, J. *Angew. Chem., Int. Ed.* **2006**, *45*, 7818–7821. (g) Liu, X.; Shang, X.; Tang, T.; Hu, N.; Pei, F.; Cui, D.; Chen, X.; Jing, X. *Organometallics* **2007**, *26*, 2747–2757. (h) Amgoune, A.; Thomas, C. M.; Carpentier, J.-F. *Macromol. Rapid Commun.* **2007**, *28*, 693–697. (i) Ma, H.; Spaniol, T. P.; Okuda, J. *Inorg. Chem.* **2008**, *47*, 3328–3339. (j) Dyer, H. E.; Huijser, S.; Schwarz, A. D.; Wang, C.; Duchateau, R.; Mountford, P. *J. Chem. Soc., Dalton Trans.* **2008**, *1*, 32–35.

(18) Spassky, N.; Wisniewski, M.; Pluta, C.; LeBorgne, A. *Macromol. Chem. Phys.* **1996**, *197*, 2627–2637.

(19) (a) Bhaw-Luximon, A.; Jhurry, D.; Spassky, N. *Polym. Bull.* **2000**, *44*, 31–38. (b) Jhurry, D.; Bhaw-Luximon, A.; Spassky, N. *Macromol. Symp.* **2001**, *175*, 67–79. (c) Nomura, N.; Ishii, R.; Akakura, M.; Aoi, K. J. *J. Am. Chem. Soc.* **2002**, *124*, 5938–5939. (d) Ishii, R.; Nomura, N.; Kondo, T. *Polym. J.* **2004**, *36*, 261–264. (e) Tang, Z.; Chen, X.; Pang, X.; Yang, Y.; Zhang, X.; Jing, X. *Biomacromolecules* **2004**, *5*, 965–970. (f) Tang, Z.; Chen, X.; Yang, Y.; Pang, X.; Sun, J.; Zhang, X.; Jing, X. *J. Polym. Sci., Polym. Chem.* **2004**, *42*, 5974–5982. (g) Yang, Y.; Tang, Z.; Pang, X.; Du, H.; Chen, X.; Jing, X. *Chem. J. Chin. Univ.* **2003**, *27*, 352–355. (h) Nomura, N.; Ishii, R.; Yamamoto, Y.; Kondo, T. *Chem.—Eur. J.* **2007**, *13*, 4433–4451.

(20) (a) Ovitt, T. M.; Coates, G. W. *J. Polym. Sci., Polym. Chem.* **2000**, *38*, 4686–4692. (b) Ovitt, T. M.; Coates, G. W. *J. Am. Chem. Soc.* **2002**, *124*, 1316–1326. (c) Zhong, Z.; Dijkstra, P. J.; Feijen, J. *Angew. Chem., Int. Ed.* **2002**, *41*, 4510–4513. (d) Zhong, Z.; Dijkstra, P. J.; Feijen, J. *J. Am. Chem. Soc.* **2003**, *125*, 11291–11298.

(21) (a) Hormnirum, P.; Marshall, E. L.; Gibson, V. C.; Pugh, R. I.; White, A. J. P. *Proc. Natl. Acad. Sci. U.S.A.* **2006**, *103*, 15343–15348. (b) Du, H.; Pang, X.; Yu, H.; Zhuang, X.; Chen, X.; Cui, D.; Wang, X.; Jing, X. *Macromolecules* **2007**, *40*, 1904–1913.

(22) Atwood, D. A.; Harvey, M. J. *Chem. Rev.* **2001**, *101*, 37–52.

(23) (a) Stolt, M.; Sodergard, A. *Macromolecules* **1999**, *32*, 6412–6417. (b) Stolt, M.; Krasowska, K.; Rutkowska, M.; Janik, H.; Rosling, A.; Sodergard, A. *Polym. Int.* **2005**, *54*, 362–368.

(24) Hocking, P. J.; Marchessault, R. H. *Macromolecules* **1995**, *28*, 6401–6409.

(25) Chisholm, M. H.; Eilerts, N. W.; Huffman, J. C.; Iyer, S. S.; Pacold, M.; Phomphrai, K. *J. Am. Chem. Soc.* **2000**, *122*, 11845–11854.

(26) Eguiburu, J. L.; Fernandez-Berridi, M. J.; Cossio, F. P.; San-Roman, J. *Macromolecules* **1999**, *32*, 8252–8258.

(27) Witzke, D. R.; Narayan, R.; Kolstad, J. J. *Macromolecules* **1997**, *30*, 7075–7085.

(28) Baran, J.; Duda, A.; Kowalski, A.; Szymanski, R.; Penczek, S. *Macromol. Rapid Commun.* **1997**, *18*, 325–333.

MA802564S